Nanoscale Horizons

ROYAL SOCIETY OF CHEMISTRY

COMMUNICATION

View Article Online
View Journal

Cite this: DOI: 10.1039/d6nh00069j

Received 10th February 2026,
Accepted 30th March 2026

DOI: 10.1039/d6nh00069j

rsc.li/nanoscale-horizons

Landauer-consistent interpretation of carrier mobility in quasi-ballistic field-effect transistors: overcoming the limitations of the Y-function method

Dokyoung Lee,[ab] Minseo Cha,[a] Hyeonsik Ahn,[c] Jusung Kim[ab] and Sungho Kim *[ab]

Carrier mobility extracted from low-field electrical measurements is widely used to interpret transport in field-effect transistors; however, its physical meaning becomes ambiguous as devices approach the quasi-ballistic regime. The Y-function method, although numerically robust, implicitly assumes drift–diffusion transport and attributes deviations in measured characteristics solely to gate-field-dependent mobility degradation. Here, we show that this assumption leads to a systematic breakdown of mobility interpretation in short-channel devices, even when polynomial Y-function analysis remains numerically stable. Temperature-dependent analysis of linear-regime transfer characteristics demonstrates that conventional Y-function-based extraction yields unphysical mobility attenuation parameters as transport departs from the diffusive limit. These anomalies do not arise from fitting instability or enhanced scattering, but from neglecting finite channel-length and injection-limited effects inherent to quasi-ballistic transport. By reinterpreting Y-function-extracted mobility within the Landauer transport formalism, we introduce a Landauer-consistent framework that explicitly separates scattering-limited mobility from ballistic constraints imposed by finite channel length. This minimal correction restores physically meaningful mobility parameters and enables self-consistent reproduction of both drain current and transconductance across the diffusive-to-quasi-ballistic transition, establishing a physically grounded approach for mobility analysis beyond the conventional applicability of the Y-function method.

New concepts

This study presents a fundamentally new, transport-regime-aware interpretation of carrier mobility extracted from low-field electrical measurements, establishing a Landauer-consistent framework for mobility analysis in nanoscale field-effect transistors. We demonstrate that mobility obtained using conventional drift–diffusion-based techniques, including the widely used Y-function method, cannot be interpreted as a purely scattering-limited material property when the channel length approaches the carrier mean free path. Instead, the experimentally extracted mobility inherently merges intrinsic scattering and injection-limited constraints imposed by finite channel length, as dictated by the Landauer formalism. Unlike previous studies that attribute anomalies in mobility extraction to field-dependent scattering, numerical instability, or empirical fitting limitations, this work explicitly identifies finite channel-length effects as the missing physical mechanism responsible for non-physical mobility attenuation parameters in the quasi-ballistic regime. By introducing a minimal, gate-voltage-independent Landauer correction without altering the core Y-function methodology or adding fitting degrees of freedom, we establish the first physically consistent separation of scattering-limited and ballistic transport contributions within a standard mobility extraction framework. This concept provides a new paradigm for interpreting electrical transport metrics and delivers critical insight for mobility analysis in emerging nanoscale materials and ultra-scaled devices where quasi-ballistic transport is unavoidable.

1. Introduction

Carrier mobility is a central parameter for interpreting the low-field transport in field-effect transistors (FETs), governing the drain current, transconductance, and overall device performance.[1] However, in practice, mobility is not a directly measured observable but an interpreted parameter whose physical meaning depends critically on the transport framework assumed in the analysis. As device dimensions are scaled to the deep nanoscale regime, carrier transport increasingly departs from the classical drift–diffusion limit due to strong confinement, enhanced electric fields, and finite channel-length effects.[2,3] Under these conditions, it becomes essential to reassess whether mobility parameters extracted from conventional low-field electrical measurements retain a clear and physically meaningful interpretation.

Among the various mobility extraction techniques, the Y-function method has been widely adopted because it enables robust parameter extraction with reduced sensitivity to series

[a] Division of Electronic and Semiconductor Engineering, Ewha Womans University, Seoul 03760, Republic of Korea. E-mail: sunghok@ewha.ac.kr
[b] Institute for Multiscale Matter and Systems (IMMS), Ewha Womans University, Seoul 03760, Republic of Korea
[c] Department of Electronic Engineering, Hanbat National University, Daejeon 34158, Republic of Korea

resistance and threshold-voltage uncertainty.[4] By exploiting the ratio between the linear-regime drain current and transconductance, the Y-function method has been successfully applied to a broad range of advanced device architectures (*e.g.*, FinFETs and fully depleted SOI FETs)[5–7] as well as non-silicon material systems, including two-dimensional semiconductors (*e.g.*, graphene, MoS_2).[8–13] To further improve the numerical stability and reduce the bias-range dependence, the polynomial Y-function method has been proposed and demonstrated to provide reliable fitting performance over extended gate-voltage ranges.[14,15] Despite these methodological refinements, all Y-function-based approaches share a common implicit assumption that low-field carrier transport can be adequately described within a drift–diffusion framework.[16]

Within this framework, deviations from the ideal Y-function behavior are interpreted exclusively in terms of the gate-field-dependent mobility degradation associated with scattering mechanisms.[4,14] This kind of interpretation is appropriate for long-channel devices operating in the diffusive regime, where the channel length significantly exceeds the carrier mean free path. However, as the channel length approaches the mean free path, finite channel-length effects and injection-limited transport can impose an intrinsic limitation on the current flow that is independent of the scattering strength.[3] In this quasi-ballistic regime, the apparent mobility inferred from electrical measurements no longer reflects a purely scattering-limited quantity, raising fundamental questions about the physical validity of the mobility parameters extracted using drift–diffusion-based techniques.

The Landauer transport formalism provides a physically transparent framework for describing the low-field transport in nanoscale devices by treating current flow as a transmission process through a finite-length channel, and has been successfully applied to a variety of device structures, including FETs,[17–19] Schottky diodes,[20] resonant tunneling devices,[21] and quantum point contacts.[22] Within this picture, two independent length scales govern transport: the carrier mean free path (λ), which characterizes scattering within the channel, and the channel length (L) itself, which sets an injection-limited upper bound on conductance even in the absence of scattering. Nevertheless, when the experimental current–voltage characteristics are interpreted using a drift–diffusion-like mobility description, these two limitations are inevitably combined into an apparent mobility that differs fundamentally from the intrinsic scattering-limited mobility.[3,19] Despite its relevance to ultra-scaled devices, this distinction has not been explicitly incorporated into conventional Y-function-based mobility analyses.

In this study, we investigate the physical meaning of the mobility extracted using the Y-function method as carrier transport enters the quasi-ballistic regime. By analyzing the temperature-dependent linear-regime transfer characteristics of a short-channel silicon FET, we show that the Y-function analysis, although numerically stable, yields systematically nonphysical mobility attenuation parameters as the transport departs from the diffusive limit. These anomalies do not originate from fitting instability, experimental uncertainty, or enhanced scattering but instead reflect the neglection of the finite channel-length and injection-limited effects inherent to quasi-ballistic transport.

To resolve this inconsistency, we reinterpret the Y-function-extracted mobility within a Landauer-consistent transport framework. By explicitly separating the scattering-limited mobility from ballistic constraints imposed by a finite channel length, we introduce a minimal correction to the conventional Y-function mobility model, which restores a physically meaningful interpretation of mobility-related parameters. More importantly, this approach does not introduce a new variant of the Y-function method. Instead, it clarifies the valid role of the Y-function in threshold-voltage extraction and supplements it with a Landauer-consistent transport model for mobility analysis. Using this framework, we demonstrate the self-consistent reproduction of both drain current and transconductance across a diffusive-to-quasi-ballistic transition with a single set of physically constrained parameters.

The results presented here establish that even modest quasi-ballistic contributions far from the fully ballistic limit can significantly distort the mobility interpretation when analyzed within a purely drift–diffusion framework. By explicitly identifying the origin of this distortion and providing a physically grounded correction, this work offers a general framework for the mobility analysis of nanoscale FETs operating beyond the conventional applicability of the Y-function method.

2. Mobility analysis with the Y-function method

2.1. Temperature-dependent transfer characteristics of a short-channel Si FET

Fig. 1 shows the measured transfer characteristics of a silicon bulk FET with a physical gate length (L) of 65 nm and channel width (W) of 2 μm (see Methods), together with the corresponding transconductance extracted from the same dataset. All measurements were performed in the linear regime using a small drain bias of V_D = 0.1 V, ensuring that the measured drain current (I_D) and transconductance (g_m) predominantly reflect low-field transport in the channel. As the temperature is reduced from 250 to 12 K, I_D increases systematically over the entire gate-voltage (V_G) range, which is consistent with the suppression of phonon scattering and the resulting enhancement of carrier transport. At the same time, the subthreshold slope becomes steeper at lower temperatures, reflecting the reduced thermal broadening of the carrier distribution and improved electrostatic control of the channel. Although dopant freeze-out may occur in the bulk at cryogenic temperatures, its impact on the present measurements is expected to be limited, since device operation is dominated by the inversion layer, where dopants are effectively fully ionized due to strong field-assisted ionization (see Section 5.3 for details).

The corresponding g_m–V_G characteristics are shown in Fig. 1b. The peak g_m increases markedly with decreasing temperature, indicating enhanced current modulation efficiency at reduced temperatures. While the overall shape of the g_m–V_G curves

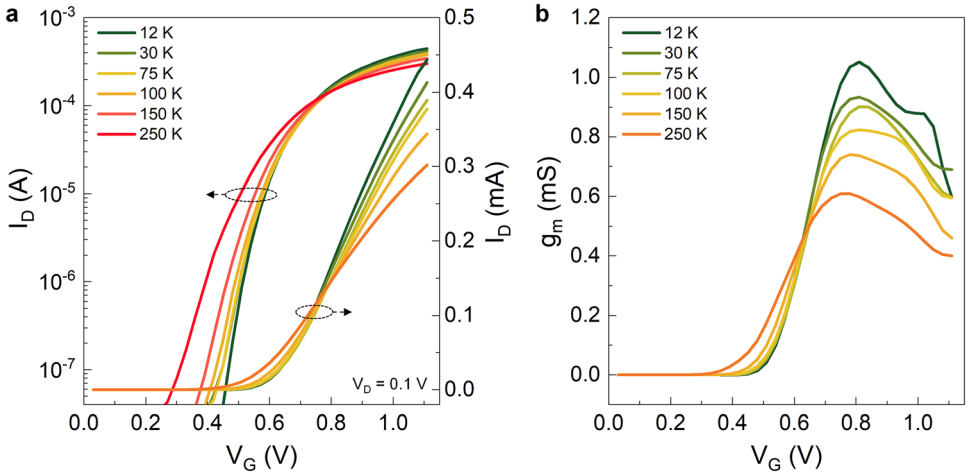

Fig. 1 Temperature-dependent linear-regime transfer characteristics of a short-channel Si bulk FET. (a) I_D as a function of V_G measured at temperatures from 250 to 12 K under a fixed drain bias (V_D) of 0.1 V. (b) Corresponding transconductance (g_m) extracted from the same I_D–V_G data, showing an increase in peak magnitude and a temperature-dependent shift of the g_m maximum as temperature decreases.

remains qualitatively similar across the investigated temperature range, both the magnitude and position of the g_m peak exhibit pronounced temperature dependence. These trends highlight the strong influence of temperature on the apparent transport behavior of this ultra-scaled device.

A channel length of 65 nm was deliberately selected to probe a transport regime that is highly sensitive to temperature-dependent variations in carrier scattering. At room temperature, this channel length is sufficiently long for the transport to be predominantly diffusive, such that drift–diffusion-based mobility descriptions remain approximately valid. As the temperature is lowered, the carrier mean free path (λ) increases and becomes comparable to the channel length (L), progressively enhancing the contribution of quasi-ballistic transport. This temperature-driven crossover provides a stringent experimental test of whether mobility parameters extracted using drift–diffusion-based analysis methods retain a clear physical interpretation once finite channel-length effects become non-negligible.

2.2. Polynomial Y-function analysis and temperature dependence of extracted mobility parameters

The polynomial Y-function method extends the conventional Y-function approach by retaining the full field-dependent mobility attenuation model while reformulating the Y-function into a polynomial form, thereby enabling the bias-range-independent extraction of mobility-related parameters (see Supplementary Notes 1 and 2).[14] Within this framework, the linear-regime drain current is interpreted using a drift–diffusion-based transport model in which the apparent mobility is expressed phenomenologically as a function of the effective gate overdrive voltage:[23]

$$\mu_{app} = \frac{\mu_0}{1 + \theta_1 V_{Gt} + \theta_2 (V_{Gt} - \Delta V_T)^2}, \quad (1)$$

where $V_{Gt} = V_G - V_T - V_D/2$ denotes the effective gate drive voltage; μ_0 is the low-field mobility; θ_1 and θ_2 are first- and second-order mobility attenuation coefficients, respectively; and ΔV_T accounts for the delayed onset of higher-order scattering mechanisms. Substituting eqn (1) into the linear-regime drain current expression yields

$$I_D = \frac{G_m V_{Gt}}{1 + \theta_1 V_{Gt} + \theta_2 (V_{Gt} - \Delta V_T)^2}, \quad (2)$$

where $G_m = (W/L)\mu_0 C_{ox} V_D$. The polynomial Y-function procedure provides a more numerically robust means of extracting the parameters $\{\mu_0, \theta_1, \theta_2, \Delta V_T\}$ in eqn (2) than the conventional Y-function method, without modifying the underlying transport assumption (Supplementary Note 2).

Fig. 2a compares the measured transfer characteristics with the curves reconstructed using the parameter sets extracted using the polynomial Y-function method. At high temperatures, the reconstructed characteristics closely reproduce the experimental data over the entire V_G range. However, as the temperature decreases, systematic deviations emerge in the strong-inversion regime. In particular, at the lowest temperature (T = 12 K), the polynomial Y-function model underestimates the measured I_D at high-V_G, indicating a progressive breakdown of the assumed transport description under these conditions. This trend is more clearly observed in the corresponding g_m characteristics, as shown in Fig. 2b. While the extracted parameters accurately reproduce the measured g_m–V_G characteristics at high temperatures, pronounced discrepancies develop at low temperatures, particularly in the high-V_G regime. The simultaneous degradation of both I_D and g_m reconstruction in the high-V_G and low-temperature regimes indicates that the observed discrepancies cannot be attributed to numerical instability, temperature-dependent fitting artifacts, contact-resistance effects, or noise amplification associated with the numerical differentiation of g_m. Instead, they indicate a fundamental limitation of the drift–diffusion-based transport assumption itself, under which all deviations from the ideal Y-function behavior are only attributed to gate-field-dependent mobility degradation.

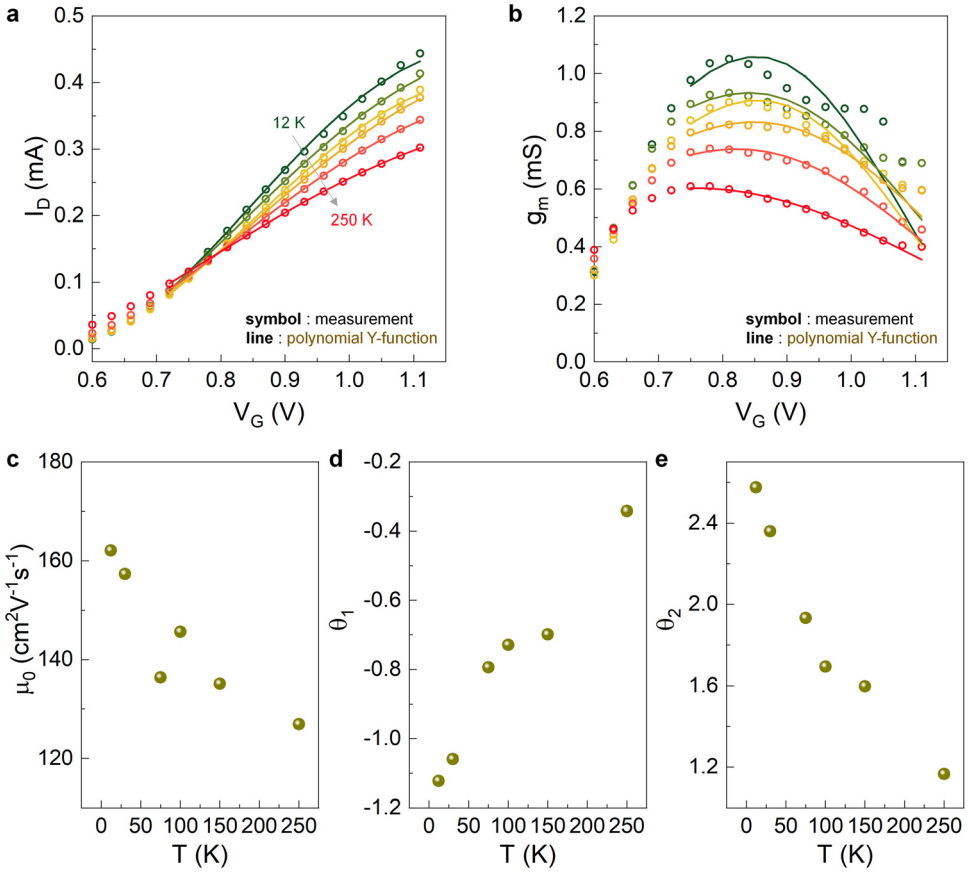

Fig. 2 Polynomial Y-function analysis of temperature-dependent transfer characteristics. (a) Measured I_D as a function of V_G, together with curves reconstructed using the parameter sets extracted by the polynomial Y-function method. (b) Corresponding g_m reconstructed from the same parameter sets and compared with the measured g_m. (c)–(e) Temperature dependence of the mobility-related parameters extracted using the polynomial Y-function method: (c) low-field mobility prefactor μ_0, (d) first-order mobility attenuation coefficient θ_1, and (e) second-order mobility attenuation coefficient θ_2.

Fig. 2c–e depict the temperature dependence of the mobility-related parameters extracted using the polynomial Y-function method. The low-field mobility μ_0 decreases monotonically with increasing temperature (Fig. 2c), consistent with conventional expectations for scattering-limited transport dominated by phonon scattering.[1] In contrast, the first-order mobility attenuation coefficient θ_1 assumes negative values over the entire temperature range (Fig. 2d). A negative θ_1 formally implies an enhanced carrier mobility with increasing transverse electric field, directly contradicting established scattering mechanisms such as phonon and surface roughness scattering, which universally lead to mobility degradation with increasing gate-field.[24,25] The second-order coefficient θ_2 remains positive (Fig. 2e); however, its pronounced temperature dependence is inconsistent with its conventional association with surface roughness scattering, which is generally only weakly dependent on temperature.[25]

Notably, the anomalous behaviors of θ_1 and θ_2 emerge concurrently and become increasingly pronounced as the temperature is reduced, indicating a common underlying origin rather than independent fitting artifacts associated with individual parameters. Altogether, these results indicate that, although the Y-function method provides a reliable numerical description of the transfer characteristics, the physical interpretation of the extracted mobility attenuation parameters becomes ambiguous in short-channel devices as transport departs from the drift–diffusion framework. This ambiguity arises because, in the quasi-ballistic regime, the apparent mobility degradation inferred from the Y-function analysis does not necessarily reflect enhanced scattering within the channel but may instead encode finite channel length and injection-limited transport effects that are not captured by the conventional Y-function mobility model. This observation motivates a re-examination of the Y-function-extracted mobility within a transport framework that explicitly accounts for quasi-ballistic effects. This is discussed in the following section.

3. Landauer-consistent mobility and transport model

3.1. Necessity of a Landauer-based interpretation of Y-function-extracted mobility

The anomalies discussed in Section 2 indicate that the breakdown of the Y-function analysis originates not from numerical

instability but from a more fundamental inconsistency in how mobility is interpreted when transport departs from the diffusive limit. In this regime, the low-field current can no longer be fully described as a local drift governed by a field-dependent mobility. Instead, a transport framework that explicitly accounts for finite channel-length effects becomes necessary.

The Landauer transport formalism provides a physically transparent framework by describing the low-field current flow as a transmission process across a finite-length channel (see Supplementary Note 3).[26] In this picture, transport is fundamentally characterized in terms of transmission and conductance, rather than mobility.[27,28] Two independent physical length scales govern current flow: the carrier mean free path (λ), which reflects scattering within the channel, and the channel length (L), which imposes an intrinsic constraint on carrier transmission even in the absence of scattering. Nevertheless, when experimental low-field current–voltage characteristics are interpreted using a drift–diffusion-like mobility expression, these two transport limitations are inevitably conflated into a single apparent mobility. Consequently, the mobility extracted from electrical measurements no longer represents a purely scattering-limited quantity but encodes both intrinsic scattering and finite channel-length constraints.

Within this context, the relationship among the apparent mobility μ_{app}, effective (scattering-limited) mobility μ_{eff}, and ballistic mobility μ_{ball} takes a Matthiessen-like form (Supplementary Note 3),[28]

$$\frac{1}{\mu_{app}} = \frac{1}{\mu_{eff}} + \frac{1}{\mu_{ball}} \tag{3}$$

Here, μ_{eff} characterizes intrinsic scattering processes within the channel, whereas μ_{ball} represents the injection-limited upper bound on carrier transport set by the channel length and carrier injection statistics. In the present low-field, non-degenerate formulation, μ_{ball} is given by $\mu_{ball} = Lv_T/(2k_BT/q)$, where $v_T \sim T^{1/2}$ is the unidirectional thermal velocity (eqn (S3.10)). Therefore, $\mu_{ball} \sim T^{-1/2}$, indicating that its temperature dependence originates intrinsically from source injection statistics rather than from scattering processes within the channel. Eqn (3) makes it explicit that the mobility inferred from low-field electrical measurements corresponds to the apparent mobility μ_{app}, which coincides with the scattering-limited mobility μ_{eff} only in the diffusive limit where $\mu_{ball} \to \infty$. Consequently, μ_{app} in the quasi-ballistic regime cannot be interpreted solely in terms of μ_{eff}, indicating a fundamental limitation of the drift–diffusion-based mobility interpretation.

This relationship clarifies why mobility extracted using the Y-function method becomes physically ambiguous in short-channel devices, because the Y-function method implicitly interprets the mobility extracted from I_D–g_m characteristics as a scattering-limited quantity, without accounting for the finite upper bound imposed by μ_{ball}. When the Y-function method is applied without accounting for eqn (3), the finite channel-length effects are implicitly absorbed into the field-dependent mobility attenuation parameters within the drift–diffusion framework. Such misattributions provide a natural physical basis for the anomalous mobility parameters and temperature dependencies described in Section 2. Therefore, a physically meaningful interpretation of the Y-function-extracted mobility parameters in short-channel devices requires the explicit incorporation of the Landauer relationship embodied in eqn (3).

3.2. Landauer-consistent reinterpretation of mobility models used in Y-function analysis

The mobility model employed in the conventional Y-function method, introduced in eqn (1), is a phenomenological expression used to describe the mobility inferred from electrical measurements. Its functional form was constructed to capture field-dependent mobility degradation, and it implicitly assumes that the current flow is dominated by scattering processes within the channel. Therefore, eqn (1) was not derived to describe injection-limited or transmission-limited transport. Considering the Landauer-based interpretation established in Section 3.1, the mobility described by eqn (1) should instead be reinterpreted as the effective, scattering-limited mobility rather than as the apparent mobility directly inferred from electrical measurements. Within this interpretation, eqn (1) is more appropriately identified as a model for the effective mobility μ_{eff} associated solely with the intrinsic scattering processes in the channel (see also Supplementary Note 4),

$$\mu_{eff} = \frac{\mu_0}{1 + \theta_1 V_{Gt} + \theta_2 (V_{Gt} - \Delta V_T)^2} \tag{4}$$

This reinterpretation does not alter the mathematical structure of the original Y-function mobility model but clarifies the physical meaning of the extracted parameters by explicitly associating them with scattering-limited transport.

Substituting the scattering-limited mobility defined in eqn (4) into the Landauer relationship of eqn (3) yields a Landauer-consistent expression for the apparent mobility:

$$\mu_{app} = \frac{\mu_0}{1 + \theta_1 V_{Gt} + \theta_2 (V_{Gt} - \Delta V_T)^2 + \eta}, \tag{5}$$

where the dimensionless parameter $\eta = \mu_0/\mu_{ball}$ quantifies the relative importance of ballistic transport. For a given device geometry and temperature, μ_{ball} is fixed (eqn (S3.10)), whereas μ_0 represents the gate-voltage-independent low-field mobility prefactor. Consequently, η is also independent of the gate-voltage and does not introduce an additional bias-dependent degree of freedom into the mobility model. The implications of this additional gate-voltage-independent term η become evident from the limiting behavior of eqn (5). In the diffusive limit ($\mu_{ball} \to \infty$, $\eta \to 0$), eqn (5) reduces exactly to the conventional Y-function mobility model. In contrast, in the quasi-ballistic limit ($\mu_{eff} \gg \mu_{ball}$), the apparent mobility saturates toward μ_{ball} and becomes insensitive to further increases in the scattering-limited mobility μ_{eff}. Such behavior cannot be captured within a purely drift–diffusion-based mobility attenuation model. It is important to note that, although the Landauer correction term η is gate-voltage-independent, the resulting transport characteristics remain gate dependent through the field-dependent mobility attenuation terms. In particular, the apparent mobility

is determined by the combined contribution of a gate-voltage-dependent term ($\theta_1 V_{Gt} + \theta_2 V_{Gt}^2$) and a gate-voltage-independent term η in the denominator of eqn (5). As the gate overdrive increases, the relative contribution of these terms changes, leading to a gate-voltage-dependent modulation of the apparent mobility. Therefore, the manifestation of quasi-ballistic transport does not require an explicitly gate-dependent correction term, but instead emerges from the interplay between a gate-dependent scattering contribution and a gate-independent transport constraint.

The Landauer-consistent linear-regime drain current follows directly from eqn (5), as detailed in Supplementary Note 4.3.

$$I_D = \frac{G_m V_{Gt}}{1 + \theta_1 V_{Gt} + \theta_2 (V_{Gt} - \Delta V_T)^2 + \eta} \quad (6)$$

Compared with the conventional Y-function formulation, the Landauer-consistent model introduces only a single additional, gate-voltage-independent term, η. Although minimal in form, this term plays a crucial role: When quasi-ballistic transport becomes significant, finite channel-length constraints cannot be captured by adjusting the gate-field-dependent mobility attenuation coefficients alone without leading to unphysical parameter values. By explicitly separating the scattering-limited transport from the finite channel-length effects within the Y-function formalism, the Landauer-consistent model modifies the structure of the mobility attenuation function while preserving its original phenomenological basis. This formulation provides a physically well-defined framework for interpreting the mobility parameters in regimes where ballistic injection effects are non-negligible. In the following section, we assess whether this Landauer-consistent reinterpretation quantitatively accounts for the discrepancies observed in the polynomial Y-function analysis of short-channel devices.

4. Mobility analysis with a Landauer-consistent Y-function method

4.1. Fitting strategy for a Landauer-consistent transport model

The presence of the additional correction term η fundamentally alters the structure of the drain-current model, rendering the iterative polynomial Y-function fitting procedure described in Supplementary Note 2 inapplicable to mobility parameter extraction. Because η represents a gate-voltage-independent transport limitation, the total mobility attenuation can no longer be described solely as a function of the effective gate overdrive voltage (V_{Gt}). Consequently, the fundamental assumption underlying the polynomial Y-function formulation, that all deviations from ideal behavior originate from the V_{Gt}-dependent mobility degradation, breaks down. Thus, the full polynomial Y-function extraction scheme is not employed in this analysis.

Although quasi-ballistic transport necessitates a revision of the mobility interpretation, the threshold-voltage extraction remains governed by electrostatic channel formation rather than by the detailed transport mechanism. Because the Landauer correction is introduced as a gate-voltage-independent term, it does not alter the condition defining the onset of inversion. Accordingly, in our analysis, the polynomial Y-function method is used exclusively for V_T extraction and the mobility parameters are obtained using the Landauer-consistent transport model shown in eqn (6) (discussed in detail in Supplementary Note 5.3).

With V_T fixed, the measured transfer characteristics are analyzed using the Landauer-consistent drain-current model. The ballistic mobility μ_{ball} is not treated as a fitting parameter because it can be independently evaluated from the channel length and temperature within the Landauer formalism (eqn. (S3.10)). Consequently, the set of fitting parameters remains identical to that used in the conventional polynomial Y-function method, *i.e.*, $\{\mu_0, \theta_1, \theta_2, \Delta V_T\}$. The parameters are extracted using a weighted nonlinear least-squares fitting procedure that simultaneously minimizes the residuals of I_D and g_m over a common gate-voltage range in the strong-inversion regime. The simultaneous fitting of I_D and g_m ensures the internal consistency of the extracted parameters and prevents bias-dependent distortions that may occur when only a single electrical quantity is considered.

In summary, V_T is extracted independently using the polynomial Y-function method, μ_{ball} is fixed based on the Landauer formalism, and the mobility-related parameters $\{\mu_0, \theta_1, \theta_2, \Delta V_T\}$ are obtained through simultaneous fitting of I_D and g_m using the Landauer-consistent transport model.

4.2. Mobility parameters extracted using the Landauer-consistent model

Fig. 3a shows a comparison of the measured transfer characteristics with the simulated I_D reconstructed using the mobility parameters extracted from the Landauer-consistent fitting procedure described in Section 4.1. In contrast to the results obtained using the parameters extracted from the conventional polynomial Y-function method (Fig. 2a), the Landauer-consistent model accurately reproduces the measured drain current over the entire V_G range, including the high-V_G regime. This extended-range agreement reflects the ability of the modified transport model to capture the finite channel-length and injection-limited effects that become increasingly important at large gate overdrives, where a purely drift–diffusion-based interpretation of mobility is no longer sufficient.

The corresponding transconductance characteristics are shown in Fig. 3b. Using the same parameter set that reproduces I_D, the Landauer-consistent model provides a significantly improved description of g_m in the high-V_G regime compared with the polynomial Y-function results in Fig. 2b. This demonstrates that the revised mobility formulation yields a self-consistent representation of both I_D and g_m within a single physically constrained parameter set. However, at the lowest temperature (T = 12 K), residual discrepancies persist in the high-V_G region, where quasi-ballistic transport is the strongest; these deviations are discussed further in Section 5.2.

Fig. 3c–e summarize the temperature dependence of the mobility parameters extracted from the Landauer-consistent model. The low-field mobility prefactor μ_0 (Fig. 3c) decreases

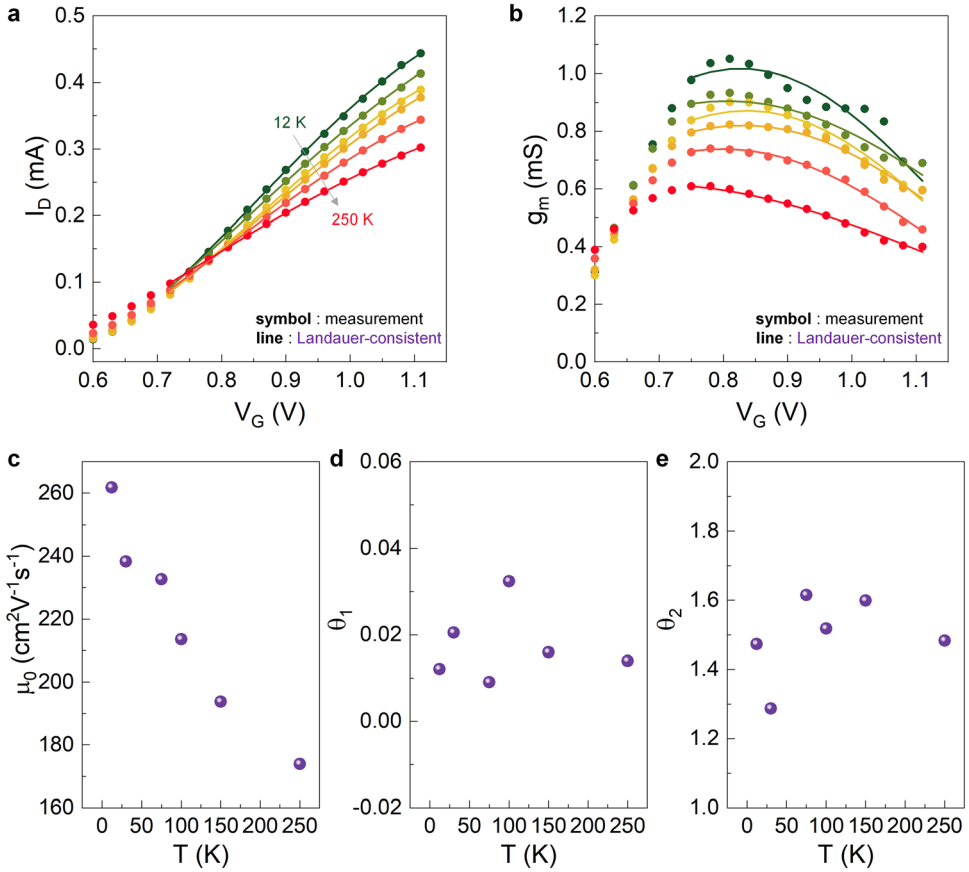

Fig. 3 Landauer-consistent analysis of temperature-dependent transfer characteristics. (a) Measured I_D as a function of V_G together with curves reconstructed using the Landauer-consistent transport model. (b) Corresponding g_m reconstructed from the same parameter sets and compared with the measured g_m. (c)–(e) Temperature dependence of the mobility-related parameters extracted using the Landauer-consistent model: (c) low-field mobility prefactor μ_0, (d) first-order mobility attenuation coefficient θ_1, and (e) second-order mobility attenuation coefficient θ_2.

monotonically with increasing temperature, consistent with the trend observed in Fig. 2c and with conventional expectations for scattering-limited transport dominated by phonon scattering. Notably, the absolute values of μ_0 obtained from the Landauer-consistent analysis are systematically larger than those extracted using the polynomial Y-function method. This difference reflects the explicit separation of the scattering-limited mobility from the finite channel-length constraints in the Landauer-based framework, which prevents the quasi-ballistic transport from being inadvertently folded into the extracted mobility prefactor.

A pronounced qualitative difference emerges in the behavior of the first-order mobility attenuation parameter θ_1, as shown in Fig. 3d. In contrast to the results obtained using the polynomial Y-function method (Fig. 2d), θ_1 is positive over the entire temperature range and exhibits no discernible temperature dependence while remaining very small in magnitude. This behavior indicates that when quasi-ballistic transport effects are explicitly accounted for through the Landauer correction term η, field-dependent scattering plays only a minor role in determining the apparent mobility. Instead, the dominant limitation on the apparent mobility in the present device results from the transition toward the quasi-ballistic transport regime, which is captured by η rather than by field-dependent mobility attenuation.

A similar trend is observed for the second-order mobility attenuation parameter θ_2 (Fig. 3e). The extracted θ_2 values exhibit no systematic temperature dependence, in sharp contrast to the anomalous behavior observed in Fig. 2e. This result is physically consistent with the well-established understanding that surface roughness scattering is only weakly dependent on the temperature.[25] The absence of artificial temperature dependence in θ_2 further supports the physical consistency of the Landauer-consistent mobility extraction.

Altogether, the results presented in Fig. 3 demonstrate that the mobility parameters extracted using the Landauer-consistent model not only provide a quantitatively improved reconstruction of the measured transfer characteristics but also exhibit trends that are physically reasonable and consistent with known scattering mechanisms. This is in clear contrast to the unphysical parameter behavior obtained from conventional Y-function analysis in the quasi-ballistic regime and highlights the necessity of incorporating Landauer-based transport considerations when interpreting the mobility in ultra-scaled FETs.

5. Discussion

5.1. Impact of Landauer correction on the breakdown of conventional Y-function analysis

The results presented in Sections 2–4 indicate that the breakdown of the conventional Y-function method in the present short-channel device does not originate from numerical instability or insufficient fitting robustness but from an incomplete transport description that neglects finite channel-length effects. Fig. 4 provides further quantitative insights into this conclusion by explicitly decomposing the apparent mobility into scattering-limited and ballistic components and clarifying why even a small Landauer correction can lead to pronounced distortions in the Y-function-extracted mobility parameters.

Fig. 4a compares the temperature dependence of the ballistic mobility μ_{ball}, effective (scattering-limited) mobility μ_{eff}, and apparent mobility μ_{app}. As expected from the Landauer formalism, μ_{ball} increases monotonically with decreasing temperature (eqn (S3.10)). This behavior does not arise from a reduction in scattering, but from the intrinsic temperature dependence of the injection velocity entering the Landauer conductance prefactor: since $v_T \sim T^{1/2}$, the corresponding ballistic mobility follows $\mu_{ball} \sim T^{-1/2}$. Thus, the increase in μ_{ball} at low temperature reflects a relaxation of the injection-limited constraint imposed by the finite channel length. In contrast, μ_{eff} exhibits a much weaker temperature dependence, decreasing with increasing temperature in a manner consistent with phonon-dominated scattering. μ_{app} remains systematically lower than μ_{eff} over the entire temperature range, indicating that our device does not operate in the fully ballistic regime.

The influence of quasi-ballistic transport is quantified by the Landauer correction term $\eta = \mu_0/\mu_{ball}$, as shown in Fig. 4b. Notably, η remains on the order of 0.05–0.12 across the investigated temperature range, indicating that the ballistic contribution constitutes only a relatively small fraction of the total mobility. Despite its small magnitude, η enters the apparent mobility as a gate-voltage-independent term in the denominator of the Landauer-consistent mobility expression (eqn (5)). Because the Y-function framework can account only for gate-voltage-dependent mobility attenuation (θ_1 and θ_2), gate-voltage-independent transport cannot be accommodated within the conventional formulation. Therefore, when the Landauer correction is omitted, the fitting procedure is forced to absorb this missing gate-voltage-independent offset into θ_1 and θ_2, leading to negative θ_1 values and anomalous temperature dependences of θ_2, as observed in Fig. 2.

Further insight is obtained from the effective transport length λ_{eff}, shown in Fig. 4c. It should be emphasized that λ_{eff} is not a directly measured microscopic mean free path, but a transport length inferred from the mobility decomposition within the Landauer-consistent framework (eqn (S3.11)), defined as $\lambda_{eff} \equiv L \cdot \mu_{eff}/\mu_{ball}$. Accordingly, λ_{eff} reflects the relative contribution of scattering-limited transport with respect to the ballistic limit, rather than the actual distance between individual scattering events. The extracted λ_{eff} decreases with decreasing temperature and remains smaller than the physical channel length (L = 65 nm) over the entire temperature range, indicating that the device does not reach the fully ballistic limit. This trend is governed by the relative temperature dependences of μ_{eff} and μ_{ball}. Although μ_{eff} increases at lower temperature due to the suppression of phonon scattering, μ_{ball} increases more strongly because it is determined by the injection-limited ballistic transport term, which follows the temperature dependence of the thermal velocity. As a result, the ratio μ_{eff}/μ_{ball}

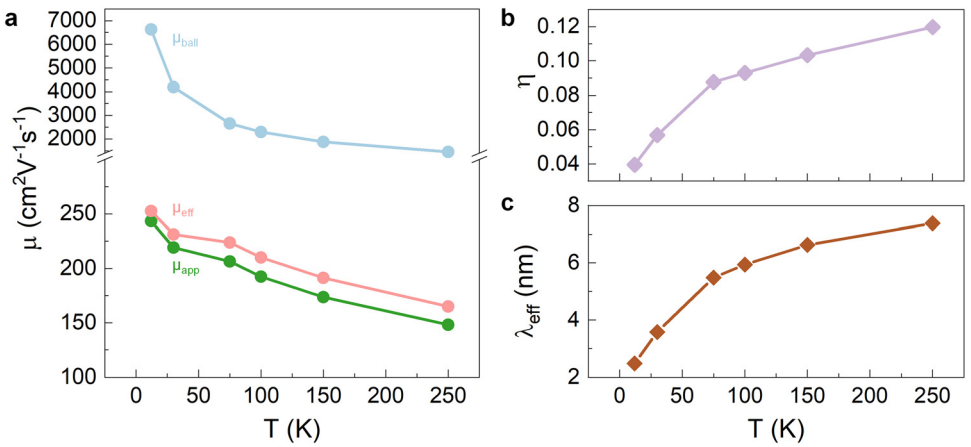

Fig. 4 Decomposition of apparent mobility and Landauer correction parameters. All quantities in (a)–(c) were evaluated at a fixed effective gate overdrive V_{Gt} to ensure comparison under equivalent inversion conditions. The reference V_{Gt} was defined from the transfer characteristic measured at T = 12 K with V_G = 1 V and was applied consistently to all temperatures using independently extracted threshold voltages $V_T(T)$. This procedure eliminates bias-induced variations in inversion charge and transverse electric field, allowing the observed temperature dependence to be attributed to intrinsic transport effects. (a) Temperature dependence of the ballistic mobility μ_{ball}, effective (scattering-limited) mobility μ_{eff}, and apparent mobility μ_{app} at a fixed effective gate overdrive V_{Gt}. (b) Temperature dependence of the Landauer correction parameter $\eta = \mu_0/\mu_{ball}$. (c) Temperature dependence of the effective transport length λ_{eff}, defined from the mobility ratio $\lambda_{eff} \equiv L \cdot \mu_{eff}/\mu_{ball}$, as extracted from the Landauer-consistent mobility analysis (eqn (S3.11)). This quantity should be interpreted as a transport length inferred from the mobility decomposition within the Landauer framework, rather than as a directly measured microscopic mean free path.

decreases upon cooling, leading to a corresponding reduction in the extracted λ_{eff}. Importantly, this behavior does not weaken the necessity of the Landauer correction. Rather, it clarifies that the central issue is not whether the device reaches the fully ballistic limit, but whether a finite channel-length effect remains present and competes with scattering-limited transport. Even when $\lambda_{eff} \ll L$, the finite channel length still gives rise to the ballistic mobility term μ_{ball}, which imposes a gate-voltage-independent transport constraint within the Landauer framework. Consequently, the apparent mobility obtained from the conventional Y-function analysis is systematically influenced by this finite-length contribution, leading to a qualitative misinterpretation of the extracted mobility attenuation parameters if it is analyzed solely within the drift-diffusion picture. Therefore, a Landauer-consistent interpretation is required whenever finite channel-length effects remain non-negligible, regardless of whether the device has entered the fully ballistic regime.

5.2. Limitations and scope of the present Landauer-consistent framework

Several limitations and scope conditions of the present Landauer-consistent mobility framework should be acknowledged to place the results of this study in the appropriate context. One direct manifestation of the restricted modeling scope adopted here is the residual mismatch observed in g_m at the lowest temperatures (Fig. 3b). This behavior should be regarded as a natural consequence of the underlying assumptions rather than as a failure of the Landauer-consistent interpretation of mobility. Unlike I_D, g_m represents the gate-voltage derivative of the current and therefore intrinsically amplifies the sensitivity to physical effects that may only weakly perturb the absolute current. Consequently, deviations arising from subtle transport or electrostatic effects tend to appear first and most prominently in g_m. Thus, physical mechanisms such as energy-dependent transmission, quantum capacitance, or changes in sub-band occupancy can produce disproportionately large deviations in g_m while leaving I_D comparatively unaffected.

In addition, this analysis is intentionally restricted to low-field transport in the linear regime, where the mapping between the Landauer conductance and an effective drift–diffusion-like mobility remains physically meaningful. Accordingly, high-field short-channel effects, such as drain-induced barrier lowering, velocity overshoot, and channel-length modulation are not considered. In addition, several physical phenomena that can become increasingly relevant at cryogenic temperatures are deliberately excluded from this framework, including impurity freeze-out, interface-state dynamics, quantum confinement, and energy-dependent transmission.[29,30] Although these effects can influence carrier transport and charge modulation, they are expected to have a stronger impact on g_m than on I_D. Therefore, the increasing g_m discrepancy observed at the lowest temperatures is consistent with the omission of these effects and does not undermine the validity of the present Landauer-consistent framework within its intended operating regime.

Another important limitation of the present framework is the neglect of parasitic contributions such as series resistance and contact resistance.[31] These parasitics primarily affect the absolute scaling of I_D and g_m and may introduce quantitative uncertainty in the extracted mobility parameters. However, they do not alter the central physical conclusion of this work, namely that the finite channel-length and injection-limited effects fundamentally modify the interpretation of the mobility extracted using drift–diffusion-based techniques in the quasi-ballistic regime. Therefore, the Landauer-consistent framework developed here is not intended as a comprehensive device model, but as a transport-regime-aware interpretation tool that clarifies the physical meaning of the mobility parameters extracted from low-field electrical measurements.

Despite these limitations, the proposed framework has several advantages. It enables physically consistent mobility analysis using only linear-regime transfer characteristics without requiring additional device structures or specialized measurement techniques. By explicitly separating scattering-limited mobility from finite channel-length constraints, the approach allows direct evaluation of physically meaningful quantities such as the Landauer correction parameter η and the effective mean free path λ. Within its defined scope, the present Landauer-consistent framework provides a robust and experimentally accessible basis for mobility interpretation in nanoscale FETs, particularly under cryogenic and quasi-ballistic operating conditions.

Finally, the present framework assumes an energy-averaged transport description in which the mean free path and mobility can be represented by effective scalar quantities. This approximation is appropriate for the near-equilibrium, low-field transport conditions considered in this study. However, in emerging material systems such as two-dimensional semiconductors or graphene, where the mean free path and transmission can exhibit strong energy dependence due to non-parabolic band structures and complex density-of-states characteristics, a more general treatment may be required. In such cases, the transport should be described using an energy-resolved Landauer formulation, and the mobility may no longer be represented by a single effective parameter. Nevertheless, the central concept of the present work, the separation between scattering-limited transport and an injection-limited constraint imposed by finite channel length, remains applicable. Extending the present framework to incorporate energy-dependent transport represents an important direction for future research.

5.3. Influence of dopant freeze-out and impurity scattering on inversion-layer transport at cryogenic temperatures

At cryogenic temperatures, incomplete dopant ionization can give rise to freeze-out effects in the bulk semiconductor, leading to a reduced density of thermally activated carriers. In conventional bulk transport, such effects are often accompanied by an increased influence of charged impurity scattering, which can become a dominant mobility-limiting mechanism as phonon scattering is suppressed. However, in FET operation, carrier transport in the linear regime is governed primarily by the inversion layer formed near the semiconductor surface, rather than by the bulk carrier population. It is therefore essential to distinguish between bulk and surface ionization under electrostatic gating. Even at deep-

cryogenic temperatures, the dopant ionization probability near the surface rapidly approaches unity as the surface potential exceeds the flat-band condition due to strong field-assisted ionization.[29] As the surface bands bend under gate bias, the relative alignment between the dopant energy levels and the quasi-Fermi level shifts, resulting in a rapid transition from incomplete to nearly complete ionization in the channel region. Consequently, under strong-inversion conditions relevant to the present measurements, the dopants in the vicinity of the channel can be regarded as effectively fully ionized.

This has important implications for scattering mechanisms. Although charged impurity scattering is intrinsically associated with ionized dopants, its effectiveness in the inversion layer is substantially reduced due to electrostatic screening by the high density of gate-induced carriers. In addition, the spatial separation between the inversion charge centroid and the bulk dopants further weakens the Coulomb interaction. As a result, the contribution of charged impurity scattering to the overall mobility is suppressed compared to bulk transport, even at low temperatures. Under these conditions, carrier transport is predominantly governed by mechanisms associated with the inversion layer, such as phonon scattering and surface-related scattering processes. Consistent with this picture, the experimentally extracted low-field mobility exhibits a monotonic decrease with increasing temperature, indicating that phonon scattering remains the dominant temperature-dependent mechanism. No signatures of impurity-scattering-limited transport, such as mobility saturation or anomalous temperature trends at low temperatures, are observed.

Therefore, although partial dopant freeze-out and impurity scattering may exist in the bulk, their influence on the inversion-layer charge and the measured drain current is negligible. The transport characteristics analyzed in this study are primarily determined by gate-induced carriers and remain well described by a mobility-based framework. This supports the interpretation that the observed increase in drain current with decreasing temperature is predominantly governed by reduced phonon scattering, rather than by variations in dopant ionization or impurity scattering.

6. Conclusion

In this study, we have examined the physical meaning of carrier mobility extracted from low-field electrical measurements in FETs as carrier transport enters the quasi-ballistic regime. We have shown that mobility is not a purely intrinsic material property directly revealed by electrical measurements but an interpreted quantity whose meaning depends critically on the underlying transport framework. As the channel length becomes comparable to the carrier mean free path, the finite channel-length and injection-limited effects increasingly influence the current flow, rendering conventional drift-diffusion-based mobility interpretations ambiguous.

By applying a polynomial Y-function analysis to temperature-dependent linear-regime transport characteristics, we have demonstrated that Y-function-based mobility extraction, although numerically robust, systematically yields nonphysical mobility attenuation parameters as transport departs from the diffusive limit. Importantly, these anomalies do not originate from fitting instability, experimental uncertainty, or enhanced scattering mechanisms. Instead, they arise from the implicit drift–diffusion assumption embedded in the Y-function-based analysis, which fails to account for the intrinsic transport limitation imposed by the finite channel length in the quasi-ballistic regime.

To resolve this inconsistency, we reinterpret the Y-function-extracted mobility within the Landauer transport formalism, which explicitly incorporates the finite channel-length and injection-limited effects. This Landauer-consistent reinterpretation enables a clear separation between scattering-limited mobility and ballistic constraints imposed by the channel length, restoring a physically meaningful interpretation of mobility-related parameters. With this framework, both the drain current and transconductance can be described self-consistently using a single set of physically constrained parameters across the diffusive-to-quasi-ballistic transition.

The results presented here establish that even modest quasi-ballistic contributions far from the fully ballistic limit can significantly distort the mobility interpretation when analyzed within a purely drift–diffusion framework. By explicitly identifying the origin of this distortion and providing a physically grounded correction, this study offers a general framework for the mobility analysis of field-effect transistors operating beyond the conventional applicability of the Y-function method. More broadly, our findings highlight the necessity of a transport-regime-aware interpretation when extracting and comparing mobility in nanoscale electronic devices.

7. Methods

7.1. Device fabrication

The silicon bulk FET investigated in this study was fabricated using a commercial 65 nm low-power CMOS technology platform provided by TSMC. An n-channel MOSFET with a low-threshold-voltage (low-V_T) option was employed. The device was realized on a p-type bulk silicon substrate using a planar CMOS process flow. The gate dielectric consisted of a thermally grown SiO_2 layer with a physical thickness of 2.6 nm. The low-V_T NMOS device was designed to operate at a nominal supply voltage of 1.2 V. All fabrication steps were carried out using a standard foundry process without any post-fabrication modification or additional processing.

7.2. Electrical measurements

Electrical measurements were conducted in a cryostat, as shown in Fig. S1. Gate and drain voltages were applied, and the drain current was measured using a source-measure unit (Keysight B2902). Cryogenic measurements were performed using a Gifford–McMahon (G–M) type closed-cycle cryostat (Sumitomo RDK-415D), which operates without liquid helium. The cryostat enabled cooling to temperatures as low as approximately 4.2 K,

with cooling capacities of 35 W at 50 K for the first stage and 1.5 W at 4.2 K for the second stage.

The device was mounted on a thermally conductive sample holder made of oxygen-free high-conductivity (OFHC) copper and was mechanically attached to the second-stage cold head. All measurements were carried out under high-vacuum conditions of approximately 10^{-6} Torr. The sample temperature was monitored using temperature sensors positioned in close proximity to the device. Prior to each electrical measurement, sufficient thermal stabilization was ensured, and electrical connections were established through dedicated cryostat feedthrough ports.

Conflicts of interest

The authors declare no conflicts of interest.

Data availability

The data that support the findings of this study, including temperature-dependent electrical measurement data (I_D–V_G and g_m–V_G characteristics) and the processed datasets used for analysis and modeling, are included within the article and its supplementary information (SI). Supplementary information is available. See DOI: https://doi.org/10.1039/d6nh00069j.

Additional raw data supporting the conclusions of this work are available from the corresponding author upon reasonable request.

Acknowledgements

This work was supported by National Research Foundation of Korea (NRF) grants funded by the Korean government (MSIT and MOE) (RS-2024-00449412, RS-2025-16063688, RS-2025-00516839, RS-2025-25422065).

References

1 Y. Taur and T. H. Ning, *Fundamentals of Modern VLSI Devices*, Cambridge University Press & Assessment, 3rd edn, 2022.
2 M. Lundstrom, *IEEE Electron Device Lett.*, 1997, **18**, 361–363.
3 A. Rahman, J. Guo, S. Datta and M. S. Lundstrom, *IEEE Trans. Electron Devices*, 2003, **50**, 1853–1864.
4 G. Ghibaudo, *Electron. Lett.*, 1988, **24**, 543–545.
5 S. J. Chang, M. Bawedin and S. Cristoloveanu, *IEEE Trans. Electron Devices*, 2014, **61**, 1979–1986.
6 T. A. Karatsori, C. G. Theodorou, E. G. Ioannidis, S. Haendler, E. Josse, C. A. Dimitriadis and G. Ghibaudo, *Solid State Electron.*, 2015, **111**, 123–128.
7 A. Tsormpatzoglou, K. Papathanasiou, N. Fasarakis, D. H. Tassis, G. Ghibaudo and C. A. Dimitriadis, *IEEE Trans. Electron Devices*, 2012, **59**, 3299–3305.
8 S. Wu, Y. Zeng, X. Zeng, S. Wang, Y. Hu, W. Wang, S. Yin, G. Zhou, W. Jin, T. Ren, Z. Guo and J. Lu, *2D Mater.*, 2019, **6**, 025007.
9 S. K. Mallik, S. Sahoo, M. C. Sahu, S. K. Gupta, S. P. Dash, R. Ahuja and S. Sahoo, *J. Appl. Phys.*, 2021, **129**, 145106.
10 K. Hemanjaneyulu, J. Kumar and M. Shrivastava, *IEEE Electron Device Lett.*, 2022, **43**, 635–638.
11 D. Y. Jeon, S. Joo, D. Lee and S. Hong, *ACS Appl. Electron. Mater.*, 2023, **6**, 465–471.
12 J. Jang, Y. J. Lee, H. Roh and S. Kim, *Sci. Rep.*, 2025, **15**, 27901.
13 F. Urban, G. Lupina, A. Grillo, N. Martucciello and A. Di Bartolomeo, *Nano Express*, 2020, **1**, 010001.
14 D. Fleury, A. Cros, H. Brut and G. Ghibaudot, in IEEE International Conference on Microelectronic Test Structures, 2008, pp. 160–165.
15 D. Fleury, A. Cros, G. Bidal, J. Rosa and G. Ghibaudo, *IEEE Electron Device Lett.*, 2009, **30**, 975–977.
16 A. Tahiat, B. Cretu, A. Veloso and E. Simoen, *Solid State Electron.*, 2025, **225**, 109071.
17 M. Bttiker, Y. Imry, R. Landauer and S. Pinhas, *Phys. Rev. B: Condens. Matter Mater. Phys.*, 1985, **31**, 6207.
18 J. Wang and M. Lundstrom, *IEEE Trans. Electron Devices*, 2003, **50**, 1604–1609.
19 R. Wang, H. Liu, R. Huang, J. Zhuge, L. Zhang, D. W. Kim, X. Zhang, D. Park and Y. Wang, *IEEE Trans. Electron Devices*, 2008, **55**, 2960–2967.
20 A. Di Bartolomeo, K. Intonti, L. Peluso, R. Di Marco, G. Vocca, F. Romeo, F. Giubileo, A. Grillo and E. Orhan, *Nano Express*, 2025, **6**, 022501.
21 J. Q. You, C.-H. Lam and H. Z. Zheng, *Phys. Rev. B: Condens. Matter Mater. Phys.*, 2000, **62**, 1978.
22 B. J. Van Wees, E. M. M. Willems, C. J. P. M. Harmans, C. W. J. Beenakker, H. Van Houten, J. G. Williamson, C. T. Foxon and J. J. Harris, *Phys. Rev. Lett.*, 1989, **62**, 1181.
23 T. C. Ong, P. K. Ko and C. Hu, *IEEE Trans. Electron Devices*, 1987, **34**, 2129–2135.
24 A. Toriumi, M. Iwase and H. Tango, *IEEE Trans. Electron Devices*, 1994, **41**, 2357–2362.
25 A. Toriumi, M. Iwase and H. Tango, *IEEE Trans. Electron Devices*, 1994, **41**, 2363–2368.
26 R. Landauer, *IBM J. Res. Dev.*, 1957, **1**, 223–231.
27 S. Datta, *Lessons from Nanoelectronics: A New Perspective on Transport*, World Scientific Connect, 1st edn, 2012.
28 M. Lundstrom and C. Jeong, *Near-Equilibrium Transport: Fundamentals and Applications*, World Scientific Connect, 2013.
29 A. Beckers, F. Jazaeri and C. Enz, *IEEE Trans. Electron Devices*, 2018, **65**, 3617–3625.
30 G. Pahwa, P. Kushwaha, A. Dasgupta, S. Salahuddin and C. Hu, *IEEE Trans. Electron Devices*, 2021, **68**, 4223–4230.
31 D. W. Lin, M. L. Cheng, S. W. Wang, C. C. Wu and M. J. Chen, *IEEE Trans. Electron Devices*, 2010, **57**, 890–897.